Published in final edited form as:
J Neurosci Methods. 2008 March 15; 168(2): 373–382.

Simultaneous Nitric Oxide and Dehydroascorbic Acid Imaging by Combining Diaminofluoresceins and Diaminorhodamines

Xiaoying Ye, **Stanislav S. Rubakhin**, and **Jonathan V. Sweedler***
Department of Chemistry and the Beckman Institute, University of Illinois, Urbana, Illinois 61801

Abstract

Spatial measurements of nitric oxide (NO) production are important to understand the function and metabolism of this molecule. The reagent, 4,5-diaminofluorescein (DAF-2) and several structurally similar probes are widely used for detection and imaging of NO. However, DAF-2 also reacts with dehydroascorbic acid (DHA) in biological samples, with both products having nearly indistinguishable fluorescence spectra. Measurements using fluorimetry and fluorescence microscopy cannot easily differentiate NO-related fluorescent signals from DHA-related signals. While DAFs and the structurally related diaminorhodamines (DARs) both react with NO and DHA, they do so to different extents. We report a multiderivatization method to image NO and DHA simultaneously by using both DAF and DAR. Specifically, DAF-2 and DAR-4M are used to image NO and DHA concentrations; after reaction, the solutions are excited, at 495 nm to measure fluorescence emission from DAF-2, and at 560 nm to measure fluorescence emission from DAR-4M. Using the appropriate calibrations, images are created that depend either on the relative NO or the relative DHA concentration, even though each probe reacts to both compounds. The method has been validated by imaging NO production in both undifferentiated and differentiated pheochromocytoma cells.

Keywords

nitric oxide; dehydroascorbic acid; fluorescence imaging; DAF-2 DA; DAR-4M AM; PC12 cells

1. Introduction

The localization of molecules within cells using specialized probes and fluorescence microscopy is one of the most important tools available to study cellular function. The performance of such approaches depends on the specificity of the probe(s) used to create the images. Here we report an improved method to image nitric oxide (NO) and dehydroascorbic acid (DHA) within cells.

NO is an intracellular and intercellular messenger that governs numerous biological processes. For instance, NO regulates blood flow by adjusting the muscle tone of blood vessels (Boger, 2003; Fan et al., 1996; Gardiner et al., 1990; Kono et al., 2006). The immune system uses NO in fighting viral, bacterial and parasitic infections (Geller et al., 1993; Grzybicki et al., 1997; Nakayama et al., 1992). NO also transmits messages between nerve cells and is associated with

*Corresponding author, Department of Chemistry, University of Illinois, 600 South Mathews Ave. 63-5, Urbana, IL 61801, Voice: 217-244-7359, Fax: 217-265-6290, e-mail: sweedler@scs.uiuc.edu

the processes of learning and memory (Garthwaite and Boulton, 1995; Guix et al., 2005; Snyder and Ferris, 2000). Endogenous NO is produced by three isoforms of nitric oxide synthase (NOS): neuronal (nNOS or NOS1), inducible (iNOS or NOS2) and endothelial (eNOS or NOS3) (Alderton et al., 2001; Griffith and Stuehr, 1995; Wiesinger, 2001).

The production and local levels of NO are regulated by several mechanisms including ones involving ascorbic acid (AA). AA is a key water-soluble antioxidant in many biological systems, donating reducing hydrogen when being oxidized to DHA (Carr and Frei, 1999; May, 1998). Uptake of AA into cells appears to be via DHA as DHA is preferentially transported through the cell membrane (Agus et al., 1997). Once inside the cell, DHA is reduced to AA through enzymatic processes that involve glutathione, NADH or NADPH reductants (Deutsch, 2000). While tissues vary widely in AA/DHA content, the concentrations are often in the low millimolar range (Ek et al., 1995; Grunewald, 1993; Rice and Russo-Menna, 1998; Washko et al., 1993), with the highest concentrations in the pituitary and adrenal glands, and the brain (Grunewald, 1993). Thus, the same tissues that contain NOS enzymes have high levels of AA and DHA. As AA may potentiate NO synthesis in endothelial cells and impact endothelial NO activity (Carr and Frei, 2000; Heller et al., 1999), these two biochemical systems interact, demonstrating the need to follow both with imaging approaches. However, measuring the activity of NOS enzymes and the levels of DHA/AA is difficult due to the lack of an easily accessible and sensitive technique to measure and image NO production and DHA content directly in biological systems.

A series of fluorescent indicators for NO, developed beginning in 1998 (Kojima et al., 2001; Kojima et al., 1998; Nagano and Yoshimura, 2002), were based on 4,5-diaminofluorescein (DAF-2) and structurally similar dyes. These dyes are widely used for detection and imaging of NO because of their sensitivity and specificity (Kasim et al., 2001; Leikert et al., 2001; Strijdom et al., 2004). However, DAF-2 also reacts with DHA in biological samples to form DAF-2-DHAs. As both have similar fluorescence spectra (Zhang et al., 2002), measurements using a fluorimeter or a fluorescence microscope cannot differentiate NO-based fluorescence from DHA-based fluorescence.

Several methods to reduce these interferences have been reported by taking advantage of the differences between the two molecules. For example, because DAF-2 reacts with NO at low temperatures (Ye et al., 2004), in one method, biological tissues are frozen into microliter-volume ice blocks using dry ice and placed immediately adjacent to a frozen block of DAF-2. NO in the frozen sample diffuses into the DAF-2 block and reacts with DAF-2, but other cellular components cannot mix with the DAF-2, eliminating the confounding effects of cellular interferences. Another approach uses capillary electrophoresis (CE) to separate the DAF fluorescent products of NO from those of DHA (Kim et al., 2006). NO production in tissues and single cells has been successfully measured using these methods by fluorimetry and CE coupled with laser induced fluorescence detection. However, imaging NO production or DHA levels is impracticable using these methods.

Here we report a ratiometric imaging approach that allows both NO and DHA to be imaged using multiderivatization. Although DAF-2 and diaminorhodamine-4M (DAR-4M) both react with NO and DHA, each reacts to a different extent. Therefore, using the two dyes and appropriate calibrations at two excitation wavelengths and two emission wavelengths, NO and DHA images can be generated, here using both undifferentiated and differentiated pheochromocytoma (PC12) cells. PC12 cells are neural crest-derived cells that can be differentiated to form neuron-like cells (Belliveau et al., 2006; Greene and Tischler, 1976; Ravni et al., 2006). This cellular line contains nNOS, and NO is required for their differentiation (Hindley et al., 1997; Peunova and Enikolopov, 1995; Phung et al., 1999). Using these cells as our model, the presence of diffusely localized DHA and punctuate NO are observed.

2. Materials and methods

2.1. Chemicals and reagents

The chemicals used were of the highest available purity and obtained from Sigma-Aldrich (St. Louis, MO) unless otherwise noted. The 0.1 M phosphate buffer (pH 7.4 ± 0.1) was prepared using 0.26 g monobasic sodium phosphate ($NaH_2PO_4 \cdot H_2O$) and 2.17 g dibasic sodium phosphate ($Na_2HPO_4 \cdot 7\ H_2O$) in 100 ml ultrapure MilliQ (Billerica, MA) water. Phosphate buffer was purged with N_2 gas for 30 min to eliminate molecular oxygen before use. DAF-2 and DAF-2 DA were purchased from EMD Biosciences, Inc. (Calbiochem, La Jolla, CA). DAR-4M and DAR-4M-AM were purchased from Molecular Probes Inc. (Eugene, OR). The original fluorescent reagents, dissolved in dimethyl sulfoxide (DMSO), were diluted into phosphate buffer for fluorimeter experiments and into cell culture media for fluorescence imaging. The final concentration of these indicators in buffers was 10 μM and the final concentration of DMSO less than 1% (v/v). DHA was purchased from Fisher Scientific (Fair Lawn, NJ). DHA exists as a dimer in the crystalline form, but it spontaneously converts to a hydrated monomer in aqueous solution. DHA solutions were freshly prepared prior to each experiment. NO-saturated solution was prepared by bubbling NO gas (Matheson Gas, S. J. Smith Welding Supply, Urbana, IL) into the deoxygenated phosphate buffer. NO gas was purified by passing through a 5M NaOH solution before it was bubbled into phosphate buffer. The saturated solution is assumed to contain ~2 mM NO at room temperature (Beckman et al., 1996); this solution was diluted immediately before use to create the required NO concentrations.

2.2. Cell culture and treatments

PC12 cells were maintained in RPMI 1640 (Cambrex, East Rutherford, NJ) enriched with 2.5% fetal bovine serum (Clontech, Mountain View, CA), 7.5% horse serum (Sigma-Aldrich), 2 mM L-glutamine (Gibco, Burlington, ON, Canada), 100 U/mL penicillin (Cambrex) and 100 μg/mL streptomycin (Cambrex) at 37°C in a 5% CO_2, 20% oxygen atmosphere. The cells were passaged immediately after having reached complete confluence.

For PC12 differentiation experiments, cells were plated at a density of < 25% confluence in RPMI 1640 containing 0.25% fetal bovine serum, 0.75% horse serum, 2 mM L-glutamine, 100 units/mL penicillin, and 100 μg/mL streptomycin. The differentiation was induced using 0.16 μM 12-*o*-tetradecanoyl phorbol-13-acetate (TPA) (Sigma-Aldrich).

To maintain the cell line and to observe cells at low magnifications using fluorescence microscopy, cells were cultured in FALCON™ polystyrene Petri dishes (BD Biosciences, San Jose, CA). In situations where high resolution and magnification were required, especially with an oil immersion objective lens, cells were transferred and cultured in glass-bottomed dishes (MatTek, Ashland, MA) or directly on Nunc™ Lab-Tek™ chambered borosilicate cover glasses (Fisher).

2.3. Fluorimeter analysis

Fluorescence measurements were performed with a spectrophotometer (F-3010, Hitachi, Tokyo, Japan). The emission fluorescence of a 0.2 mL reaction mixture was monitored upon excitation at 495 nm (scan range 500-600 nm) and at 560 nm (scan range 565-650 nm). The excitation and emission bandpass were set to 5 nm. Scan speed and response time was 60 nm/min and 2 s, respectively. The fluorescence counts were calculated with Microsoft Excel 2002 (Microsoft, Redmond, WA).

2.4. Fluorescence microscope

Bright field images and fluorescence images were obtained by a Zeiss Axiovert 200M or Zeiss Axiovert 25 inverted microscope (Zeiss, Standort Gottingen, Germany). For the Axiovert 200M, a halogen lamp (100 W) and a mercury vapor lamp (150 W) were used as the light sources. Images were acquired using an electron multiplying charge-coupled device camera (Cascade 512B) (Roper Scientific, Tucson, AZ). For the Axiovert 25, a halogen lamp (25 W) and a mercury vapor lamp (50 W) were used as the light sources. Images were acquired using an AxioCam MRc camera (Zeiss). Both systems were supported by the Zeiss Axiovision software package. For each set of experiments, images were digitized under constant exposure time, gain and offset. The exposure time was less than 60 s.

2.5. Reaction protocols

A series of NO or DHA standards of known concentrations were mixed with solutions of DAF-2 or DAR-4M, as well as various mixtures of the two. Specifically, 10 μM DAF-2 and 10 μM DAR-4M were added to a series of standard solutions of NO and DHA. The reactions were carried out at room temperature for 30-35 min. The reaction products were subjected to fluorometric analysis immediately after reaction.

2.6. Fluorescence imaging of PC12 cells

The cells were incubated at 37 °C for 20 min in culture medium containing 10 μM DAF-2 DA and 10 μM DAR-4M AM for dye loading according to the method outlined by Kojima et al (Kojima et al., 2001; Kojima et al., 1998). The cells were then washed using RPMI 1640 and switched back to normal medium. The cells were analyzed under a fluorescence microscope with a green channel, an excitation of 450-490 nm and emission detection with a 515-560 nm bandpass green filter; and a red channel, an excitation of 515-560 nm and emission detection with a 590 nm longpass red filter. Control cultures were incubated with only DAF-2-DA and the cells were analyzed only with the green channel. As a negative control, cells were incubated in medium lacking DAF-2 DA or DAR-4M AM.

Pharmacological experiments were performed by incubating PC12 cells in culture medium containing an NOS inhibitor, N^G-Nitro-L-arginine methyl ester (L-NAME), for 12 h, or an NO scavenger, 2-(4-carboxyphenyl)-4, 4, 5, 5-tetramethylimidazoline-1-oxyl-3-oxide (carboxy-PTIO), for 30 min. Then the cells were incubated in the medium containing DAF-2 DA and DAF-4M AM, supplemented with drugs as described above.

2.7. Data analysis

Images in the RGB color mode were converted to grayscale by extracting green or red channel signals using ImageJ software (Wayne Rasband, NIH, Bethesda, MD). Fluorescence intensity was measured from images using ImageJ software. Multiple regression was performed by Origin 6.0 (OriginLab, Northampton, MA). Digital image processing was performed using AnalyzeAVW software (Mayo Clinic Foundation, Rochester, MN). Homoscedastic two-tailed Student's *t*-tests were applied to assess the significance of the difference using the TTEST function in Microsoft Excel 2002 and $P < 0.05$ was considered to be significant.

3. Results

3.1. DAF-2 and DAR-4M both react with NO and DHA

The reaction of DAF-2 with NO and DHA was first examined by using a fluorimeter with 495 nm excitation. Fluorescence spectra of DAF-2 with either NO or DHA are shown in Fig. 1A. DAF-2 reacts with NO, forming a fluorescent product, DAF-2-triazole (DAF-2-T). DAF-2 also reacts with DHA to form DAF-2-DHAs (Zhang et al., 2002). DAF-2-T and DAF-2-DHAs have

similar fluorescence spectra, both of which have excitation/emission maxima at 495/515 nm. Next we determined the specificity of DAR-4M with NO and DHA with 560 nm excitation (Fig. 1B). Appreciable fluorescence signal was observed from DAR-4M and DHA mixtures. The fluorescence profiles of DAR-4M-DHA showed a high degree of similarity to those from DAF-4M-triazole (DAF-4M-T) in that both have excitation/emission maxima at 560/575 nm. DAF-2 and DAR-4M have similar sensitivity to NO in spite of the differences observed in the excitation/emission maxima and the fluorescence intensity of the triazole product.

3.2. A ratiometric approach to measure NO and DHA using DAF-2 and DAR-4M

A dual dye/dual wavelength ratiometric approach is investigated to deconvolve the signals and obtain measures of each compound individually. Because the physiological levels of NO are as high as the micromolar range, and DHA levels are as high as the low millimolar range, appropriate levels were used here to create the calibrations (see Table 1). After the 30 min reaction, the products of the reaction were excited at 495 nm and the fluorescence emission from DAF products measured at 515 nm (Fig. 2A). Then the mixture was excited at 560 nm and the fluorescence emission from DAR-4M was measured at 575 nm (Fig. 2B). The fluorescence measured at 515 nm depends on both the NO concentration and the DHA concentration, as does the fluorescence intensity measured at 575 nm, but both to different extents. Thus, a system of two linear equations with two independent variables was formed according to Equation 1:

$$\begin{cases} F_{515} = a_1 + b_1 \times C_{\mathrm{DHA}} + c_1 \times C_{\mathrm{NO}} \\ F_{575} = a_2 + b_2 \times C_{\mathrm{DHA}} + c_2 \times C_{\mathrm{NO}} \end{cases} \quad \text{Eq.1}$$

where F_{515} is the fluorescence intensity at 515 nm emission with 495 nm excitation, F_{575} is the fluorescence intensity at 575 nm emission with 560 nm excitation, C_{NO} is the concentration of NO, and C_{DHA} is the concentration of DHA. a_1 and a_2 are the constants, b_1 and b_2 are the coefficients of DHA concentration, and c_1 and c_2 are the coefficients of NO concentration at emission wavelengths of 515 nm and 575 nm, respectively. The coefficients, b_1, b_2, c_1, c_2, and the constants a_1, a_2, were obtained by a multiple regression method with a series of standard solutions at different concentrations of NO and DHA. NO and DHA concentrations in unknown samples are determined as shown in Equation 2:

$$\begin{cases} C_{\mathrm{NO}} = \frac{(b_2 \times F_{515} - b_1 \times F_{575}) - (a_1 \times b_2 - a_2 \times b_1)}{c_1 \times b_2 - c_2 \times b_1} \\ C_{\mathrm{DHA}} = \frac{(c_2 \times F_{515} - C_1 \times F_{575}) - (a_1 \times c_2 - a_2 \times c_1)}{b_1 \times c_2 - b_2 \times c_1} \end{cases} \quad \text{Eq.2}$$

Table 1 contains an example calibration measured at 515 nm and 575 nm with the NO/DHA concentrations shown. Multiple regression was performed using Origin 6.0. The proposed linear regression model fit the fluorescence at 515 nm and 575 nM under different concentrations of NO and DHA (R^2 = 0.997 for both equations). The calculated values of NO and DHA concentrations from an unknown solution with 33 μM NO and 830 μM DHA were 11 μM NO and 810 μM DHA. The R^2 of the linear model, created using four datasets covering NO concentrations from 0.01 μM to 90 μM and DHA concentrations from 0.025 mM to 1 mM, is 0.991 ± 0.06 for fluorescence at 515 nm and 0.996 ± 0.03 for fluorescence at 575 nm, respectively. The relative standard deviation of NO measurements with different calibration sets is 13.9 % (e.g., 0.127 ± 0.018 μM versus the expected 0.05 μM NO, n = 3). The average standard deviation of DHA measurements is 3.0 % (0.094 ± 0.008 mM versus the expected 0.083 mM DHA, n = 2 and 0.81 ± 0.01 mM versus expected 0.83 mM DHA, n = 2).

3.3. Cellular NO and DHA fluorescence imaging using the DAF/DAR ratiometric approach

The same strategy described above was modified to image NO and DHA levels in biological samples using a fluorescence microscope. PC12 cells were incubated in 10 μM DAF-2 DA and 10 μM DAR-4M AM for dye loading. DAF-2 DA and DAR-4M AM can enter the cells

through the plasma membrane, where they are converted to DAF-2 and DAR-4M by intracellular esterase(s). The fluorescence image was first collected at 515 nm emission wavelength using 488 nm excitation (Fig. 3A). PC12 cells exhibited an overall fluorescence signal with heterogeneous distribution, and a distinctive punctate pattern of intense fluorescence signal was observed within the cytoplasm. Next, a second fluorescence image was collected at 575 nm emission wavelength using 560 nm excitation (Fig. 3B). In contrast to the green fluorescence signals at 515 nm, the overwhelming majority of PC12 cells showed bright and diffuse fluorescence at this excitation.

Calibration curves were created from a series of standard solutions containing different concentrations of NO and DHA using the same fluorescence microscopy settings, in a similar manner to the fluorimeter analysis. The coefficients and constants were obtained by multiple regression. NO concentration at each pixel was calculated using Equation 2 by AnalyzeAVW software. To convert NO concentration information into an image, pixel values in the reconstructed image were adjusted as shown in Equation 3:

$$P = \left(C_{\mathrm{NO}} - C_{\mathrm{background}}\right) \times \left(P_{\max} - P_{\mathrm{background}}\right) / \left(C_{\max} - C_{\mathrm{background}}\right) \quad \text{Eq.3}$$

where P is the pixel value in the reconstructed image, C_{NO} is the NO concentration corresponding to each pixel obtained from calibration curves, $C_{\mathrm{background}}$ is the NO concentration corresponding to background pixel values $P_{\mathrm{background}}$ in the original fluorescence image, and $C_{\max}$ is the NO concentration at the maximal fluorescence intensity $P_{\max}$ in the original fluorescence image. The reconstructed image in grayscale is shown in Fig. 3C. The diffuse background fluorescence from DHA is eliminated and a sharper image for NO production is obtained.

3.4. Observation of NO production modulation by pharmacological agents

NO production in PC12 cells was observed using the DAF/DAR ratiometric method. The fluorescence signal from PC12 cells appeared punctate in nature (Fig. 4A). The average maximal fluorescence intensity of single cells was markedly decreased by pre-incubation of cells with 1 mM L-NAME for 12 h ($P < 0.01$, n = 9 cells from 3 preparations) (Fig. 4B). In addition, fewer punctuate sources were observed in the presence of L-NAME. The localized fluorescence was abolished by pre-incubation of cells with 1 mM carboxy-PTIO for 30 min ($P < 0.001$, n = 9 cells from 3 preparations) (Fig. 4C). In three control cultures not loaded with DAF-2 DA and DAR-4M AM, only weak background fluorescence was seen and there was no specific fluorescence associated with individual cells (data not shown). NO production under the same conditions was also observed by using DAF-2 DA only (Fig. 4D, E, F) and compared with the DAF/DAR ratiometric method.

NO production in differentiated PC12 cells was imaged using the same method (Fig. 5). PC12 cells in the presence of TPA undergo dramatic morphological changes, developing several structural characteristics of mature sympathetic neurons. The fluorescence observed is punctuate in nature as observed in differentiated PC12 cells and is concentrated in the neurite-like structures extended from PC12 cells.

4. Discussion

DAF-2 is one of the most commonly employed fluorescent probes for NO detection. To complicate NO measurements in biological samples using DAF-2, DHA reacts with DAF-2 under physiologically relevant conditions to form a unique series of fluorescent products, DAF-2-DHAs (Zhang et al., 2002), which have almost the same fluorescence spectra as DAF-2-T, the fluorescent product of NO and DAF-2 (Fig. 1A). DAR-4M is another frequently

used fluorescent reagent for NO with several distinctive characteristics. For example, DAR-4M uses lower energy excitation at 560 nm, which results in less damage to biological samples.

Not surprisingly, given their similar reactive structures, DAR-4M also reacts with DHA, with the fluorescence profile of the DAR-4M-DHA product also showing high similarity to that of DAR-4M-T. In fact, the reaction of DAR-4M with DHA occurs to a greater extent than the reaction between DAF-2 and DHA. Semi-quantitative calculations based on the calibration curves of triazole fluorescence versus NO concentration indicate that 1 mM DHA with DAR-4M produced a similar fluorescence signal compared to ~100 μM NO (data not shown). In contrast, the fluorescence signal of the reaction mixture of DAF-2 with 1 mM DHA was similar to ~300 nM NO-donor NONOate (Zhang et al., 2002). An interesting possibility is that the dyes themselves, by reacting with DHA, affect levels of DHA and AA in the cell; significant DHA and AA concentration changes would alter the redox state of the cell, modify NO production by NOS, and have an effect on NO lifetime. However, the concentrations of the probes are at much lower levels than DHA and so this is considered unlikely.

As DAFs and DARs both react with NO and DHA but to different extents, and the DAF derivatized products have different fluorescent profiles from DAR derivatized products, a ratiometric method has been created to produce images of NO and DHA levels. Because DHA is ubiquitously present in many cells at micromolar to millimolar levels (Kim et al., 2002), in contrast to the nanomolar physiological levels of NO, even poor reactivity of these fluorescent reagents with DHA can generate significant fluorescence artifacts that lead to erroneous information on NO production. For a solution containing NO and DHA, their concentrations can be measured by using both DAF and DAR simultaneously. Therefore, the dual dye approach may eliminate the interference of DHA when measuring NO in samples, and allow DHA imaging without interference from NO.

We have shown that a linear regression model yields a linear calibration for the fluorescence response to different NO and DHA concentrations ($R^2 = 0.997$). The scheme is capable of measuring DHA concentrations accurately, in our case, with a 3% error. The NO measurements deviate further from the true values and can be off several-fold at lower concentrations of NO. The issue relating to NO quantitation likely occurs for two reasons. First, DHA concentrations in the standard solutions, when chosen to be similar to physiological levels, are more than 100-fold higher than those of NO. More importantly, the absolute NO levels of standard solutions are not known precisely. While a saturated NO solution can be created and diluted to lower concentrations, NO is not stable, especially under dilute conditions. This makes accurate quantitation problematic. Our results indicate that the quantitative approach is well-suited for DHA measurements and eliminates the effects of DHA on NO measurements, but is not ideal for NO quantitation in the presence of high levels of DHA. If this occurs, then other approaches may be necessary (Kim et al., 2006; Ye et al., 2004).

The major goal of this work is not quantitation but is to develop protocols for imaging either or both NO and DHA in the presence of the other compound. By using both DAF-2 and DAR-4M, fluorescence images of NO and DHA can be created. One issue encountered with NO fluorescence imaging in biological samples using the DAF/DAR ratiometric method is the intracellular sequestration of the fluorescent dyes. With the incubation conditions commonly used such as 10 μM DAF-2 DA and 10 μM DAR-4M AM, the intracellular concentration of these dyes can reach the millimolar range (Rodriguez et al., 2005). We observed strong fluorescence in PC12 cells. For example, the green fluorescence signal from DAF-2-T in PC12 cells is stronger than that from the mixture of 10 μM DAF-2 and a saturated 2 mM NO solution. The physiological range of NO production is from nanomolar to micromolar levels; thus it appears that the intracellular concentration of the dye is higher than its extracellular level in this case. Due to the accumulation of DAF-2 and DAR-4M inside the cell, calibration obtained

with 10 μM DAF-2 and 10 μM DAR-4M reflects relative NO concentrations and not absolute levels.

The punctate nature of the fluorescence from PC12 cells suggests that the fluorescence imaging of NO using the DAF/DAR ratiometric method is capable of producing sufficient spatial resolution at the subcellular level. The observation of punctate fluorescence is in agreement with previous studies on NOS detection by immunohistochemistry and histochemistry (Gonzalez-Hernandez et al., 1996; Hecker et al., 1994). NOS is found within cells in association with subcellular organelles, especially with the endoplasmic reticulum and nuclear envelope and sometimes within the Golgi apparatus, and with the mitochondrial membrane (Faber-Zuschratter and Wolf, 1994; Hecker et al., 1994; Rothe et al., 1998). NO detection using DAF-2-DA has demonstrated punctate fluorescence in cultured neurons (Chen et al., 2001) and in brain slices (Brown et al., 1999; Buskila et al., 2005). L-NAME is an inhibitor of the constitutive isoforms of NOS (Moore and Handy, 1997). In the presence of L-NAME, the average maximal fluorescence intensity of single cells greatly decreased. This result indicates that the NO observed is produced by constitutive NOS (e.g., nNOS). The punctate fluorescence seen within the cytoplasm of PC12 cells in the present study may therefore represent point sources of NO production. However, as the fluorescence does not diffuse away from the point sources even after a several-hour observation, it is more likely that these punctate sources represent sequestration of the probes rather than point sources of NO generation.

The improvement on NO fluorescence imaging using the DAF/DAR ratiometric method is noticeable in Fig. 4C and F. The NO image obtained by using DAF-2 DA only shows a high level of background fluorescence from DHA, which is evenly distributed in the cells and is not suppressed by carboxy-PTIO (Fig. 4F). The NO image acquired by using the DAF/DAR ratiometric method abolishes the fluorescence from DHA, thus the effects of the NO scavenger on NO concentration is obvious.

In differentiated PC 12 cells, individual punctate fluorescence observed at the fiber tips is brighter than the individual fluorescent puncta seen within the cell soma. This result is consistent with the immunofluorescence patterns of nNOS demonstrated in nerve growth factor differentiated PC12 cells, in which bright punctate regions of nNOS immunofluorescence was observed along the perimeter of cell soma and in the neurites (Arundine et al., 2003). An increasing number of experimental studies have implicated NO as a positive regulator in neurite outgrowth (Bicker, 2005; Poluha et al., 1997; Rialas et al., 2000). It has been shown that nNOS expression and NO production is required for the differentiation of PC12 cells (Hindley et al., 1997; Peunova and Enikolopov, 1995; Phung et al., 1999). The DAF/DAR ratiometric method provides a new approach to directly study the modulatory role of NO in PC12 cell differentiation. The fluorescence images obtained using this methodology demonstrate NO production in PC12 cells with subcellular resolution, in good agreement with the immunofluorescence patterns of nNOS in PC12 cells.

We conclude that this accessible fluorescence imaging method effectively allows imaging of relative NO production in living cells without interference from DHA, is useful for identifying nitrergic cells in biological systems, and has application to a number of studies involving cellular NO production. Lastly, this ratiometric approach can be extended to detection and imaging of other compounds and fluorescence probes with similar interference problems.

Acknowledgements

The authors gratefully thank Dr. Won-Suk Kim and Andrew Shaw for assisting with fluorimeter measurements, Jonathan Ekman for aiding with the fluorescence microscope use, and Frank Huo for supplying the pheochromocytoma (PC12) cell culture. This material is based upon work supported by the National Institute on Drug Abuse under Award No. DA018310 to the UIUC Neuroproteomics Center, and the National Institutes of Health under Award No. DE018866.

References

Agus DB, Gambhir SS, Pardridge WM, Spielholz C, Baselga J, Vera JC, Golde DW. Vitamin C crosses the blood-brain barrier in the oxidized form through the glucose transporters. J Clin Invest 1997;100:2842–8. [PubMed: 9389750]

Alderton WK, Cooper CE, Knowles RG. Nitric oxide synthases: structure, function and inhibition. Biochem J 2001;357:593–615. [PubMed: 11463332]

Arundine M, Sanelli T, Ping He B, Strong MJ. NMDA induces NOS 1 translocation to the cell membrane in NGF-differentiated PC 12 cells. Brain Res 2003;976:149–58. [PubMed: 12763249]

Beckman, JS.; Wink, DA.; Crow, JP. Methods in Nitric Oxide Research. John Wiley and Sons Ltd; Chichester, England: 1996.

Belliveau DJ, Bani-Yaghoub M, McGirr B, Naus CC, Rushlow WJ. Enhanced neurite outgrowth in PC12 cells mediated by connexin hemichannels and ATP. J Biol Chem 2006;281:20920–31. [PubMed: 16731531]

Bicker G. STOP and GO with NO: nitric oxide as a regulator of cell motility in simple brains. Bioessays 2005;27:495–505. [PubMed: 15832386]

Boger RH. When the endothelium cannot say 'NO' anymore. ADMA, an endogenous inhibitor of NO synthase, promotes cardiovascular disease. Eur Heart J 2003;24:1901–2. [PubMed: 14585247]

Brown LA, Key BJ, Lovick TA. Bio-imaging of nitric oxide-producing neurones in slices of rat brain using 4,5-diaminofluorescein. J Neurosci Methods 1999;92:101–10. [PubMed: 10595708]

Buskila Y, Farkash S, Hershfinkel M, Amitai Y. Rapid and reactive nitric oxide production by astrocytes in mouse neocortical slices. Glia 2005;52:169–76. [PubMed: 15968628]

Carr A, Frei B. Does vitamin C act as a pro-oxidant under physiological conditions? FASEB J 1999;13:1007–24. [PubMed: 10336883]

Carr A, Frei B. The role of natural antioxidants in preserving the biological activity of endothelium-derived nitric oxide. Free Radic Biol Med 2000;28:1806–14. [PubMed: 10946222]

Chen X, Sheng C, Zheng X. Direct nitric oxide imaging in cultured hippocampal neurons with diaminoanthraquinone and confocal microscopy. Cell Biol Int 2001;25:593–8. [PubMed: 11448097]

Deutsch JC. Dehydroascorbic acid. J Chromatogr A 2000;881:299–307. [PubMed: 10905713]

Ek A, Strom K, Cotgreave IA. The uptake of ascorbic-acid into human umbilical vein endothelial-cells and its effect on oxidant insult. Biochem Pharmacol 1995;50:1339–46. [PubMed: 7503781]

Faber-Zuschratter H, Wolf G. Ultrastructural distribution of NADPH-diaphorase in cortical synapses. Neuroreport 1994;5:2029–32. [PubMed: 7865737]

Fan WQ, Smolich JJ, Wild J, Yu VY, Walker AM. Nitric oxide modulates regional blood flow differences in the fetal gastrointestinal tract. Am J Physiol 1996;271:G598–604. [PubMed: 8897878]

Gardiner SM, Compton AM, Bennett T, Palmer RM, Moncada S. Control of regional blood flow by endothelium-derived nitric oxide. Hypertension 1990;15:486–92. [PubMed: 2332239]

Garthwaite J, Boulton CL. Nitric oxide signaling in the central nervous system. Annu Rev Physiol 1995;57:683–706. [PubMed: 7539993]

Geller DA, Lowenstein CJ, Shapiro RA, Nussler AK, Di Silvio M, Wang SC, Nakayama DK, Simmons RL, Snyder SH, Billiar TR. Molecular cloning and expression of inducible nitric oxide synthase from human hepatocytes. Proc Natl Acad Sci USA 1993;90:3491–5. [PubMed: 7682706]

Gonzalez-Hernandez T, Perez de la Cruz MA, Mantolan-Sarmiento B. Histochemical and immunohistochemical detection of neurons that produce nitric oxide: effect of different fixative parameters and immunoreactivity against non-neuronal NOS antisera. J Histochem Cytochem 1996;44:1399–413. [PubMed: 8985132]

Greene LA, Tischler AS. Establishment of a noradrenergic clonal line of rat adrenal pheochromocytoma cells which respond to nerve growth factor. Proc Natl Acad Sci USA 1976;73:2424–8. [PubMed: 1065897]

Griffith OW, Stuehr DJ. Nitric oxide synthases: properties and catalytic mechanism. Annu Rev Physiol 1995;57:707–36. [PubMed: 7539994]

Grunewald RA. Ascorbic-acid in the brain. Brain Res Rev 1993;18:123–33. [PubMed: 8467348]

Grzybicki DM, Kwack KB, Perlman S, Murphy SP. Nitric oxide synthase type II expression by different cell types in MHV-JHM encephalitis suggests distinct roles for nitric oxide in acute versus persistent virus infection. J Neuroimmunol 1997;73:15–27. [PubMed: 9058755]

Guix FX, Uribesalgo I, Coma M, Munoz FJ. The physiology and pathophysiology of nitric oxide in the brain. Prog Neurobiol 2005;76:126–52. [PubMed: 16115721]

Hecker M, Mulsch A, Busse R. Subcellular localization and characterization of neuronal nitric oxide synthase. J Neurochem 1994;62:1524–9. [PubMed: 7510784]

Heller R, Munscher-Paulig F, Grabner R, Till U. L-ascorbic acid potentiates nitric oxide synthesis in endothelial cells. J Biol Chem 1999;274:8254–60. [PubMed: 10075731]

Hindley S, Juurlink BH, Gysbers JW, Middlemiss PJ, Herman MA, Rathbone MP. Nitric oxide donors enhance neurotrophin-induced neurite outgrowth through a cGMP-dependent mechanism. J Neurosci Res 1997;47:427–39. [PubMed: 9057136]

Kasim N, Branton RL, Clarke DJ. Neuronal nitric oxide synthase immunohistochemistry and 4,5-diaminofluorescein diacetate: tools for nitric oxide research. J Neurosci Methods 2001;112:1–8. [PubMed: 11640952]

Kim WS, Dahlgren RL, Moroz LL, Sweedler JV. Ascorbic acid assays of individual neurons and neuronal tissues using capillary electrophoresis with laser-induced fluorescence detection. Anal Chem 2002;74:5614–20. [PubMed: 12433096]

Kim WS, Ye X, Rubakhin SS, Sweedler JV. Measuring nitric oxide in single neurons by capillary electrophoresis with laser-induced fluorescence: use of ascorbate oxidase in diaminofluorescein measurements. Anal Chem 2006;78:1859–65. [PubMed: 16536421]

Kojima H, Hirotani M, Nakatsubo N, Kikuchi K, Urano Y, Higuchi T, Hirata Y, Nagano T. Bioimaging of nitric oxide with fluorescent indicators based on the rhodamine chromophore. Anal Chem 2001;73:1967–73. [PubMed: 11354477]

Kojima H, Nakatsubo N, Kikuchi K, Kawahara S, Kirino Y, Nagoshi H, Hirata Y, Nagano T. Detection and imaging of nitric oxide with novel fluorescent indicators: diaminofluoresceins. Anal Chem 1998;70:2446–53. [PubMed: 9666719]

Kono T, Saito M, Kinoshita Y, Satoh I, Shinbori C, Satoh K. Real-time monitoring of nitric oxide and blood flow during ischemia-reperfusion in the rat testis. Mol Cell Biochem 2006;286:139–45. [PubMed: 16496212]

Leikert JF, Rathel TR, Muller C, Vollmar AM, Dirsch VM. Reliable in vitro measurement of nitric oxide released from endothelial cells using low concentrations of the fluorescent probe 4,5-diaminofluorescein. FEBS Lett 2001;506:131–4. [PubMed: 11591386]

May JM. Ascorbate function and metabolism in the human erythrocyte. Front Biosci 1998;2:d1–d10. [PubMed: 9405334]

Moore PK, Handy RL. Selective inhibitors of neuronal nitric oxide synthase--is no NOS really good NOS for the nervous system? Trends Pharmacol Sci 1997;18:204–11. [PubMed: 9226999]

Nagano T, Yoshimura T. Bioimaging of nitric oxide. Chem Rev 2002;102:1235–70. [PubMed: 11942795]

Nakayama DK, Geller DA, Lowenstein CJ, Chern HD, Davies P, Pitt BR, Simmons RL, Billiar TR. Cytokines and lipopolysaccharide induce nitric oxide synthase in cultured rat pulmonary artery smooth muscle. Am J Respir Cell Mol Biol 1992;7:471–6. [PubMed: 1384580]

Peunova N, Enikolopov G. Nitric oxide triggers a switch to growth arrest during differentiation of neuronal cells. Nature 1995;375:68–73. [PubMed: 7536899]

Phung YT, Bekker JM, Hallmark OG, Black SM. Both neuronal NO synthase and nitric oxide are required for PC12 cell differentiation: a cGMP independent pathway. Brain Res Mol Brain Res 1999;64:165–78. [PubMed: 9931481]

Poluha W, Schonhoff CM, Harrington KS, Lachyankar MB, Crosbie NE, Bulseco DA, Ross AH. A novel, nerve growth factor-activated pathway involving nitric oxide, p53, and p21WAF1 regulates neuronal differentiation of PC12 cells. J Biol Chem 1997;272:24002–7. [PubMed: 9295352]

Ravni A, Bourgault S, Lebon A, Chan P, Galas L, Fournier A, Vaudry H, Gonzalez B, Eiden LE, Vaudry D. The neurotrophic effects of PACAP in PC12 cells: control by multiple transduction pathways. J Neurochem 2006;98:321–9. [PubMed: 16805827]

Rialas CM, Nomizu M, Patterson M, Kleinman HK, Weston CA, Weeks BS. Nitric oxide mediates laminin-induced neurite outgrowth in PC12 cells. Exp Cell Res 2000;260:268–76. [PubMed: 11035921]

Rice ME, Russo-Menna I. Differential compartmentalization of brain ascorbate and glutathione between neurons and glia. Neuroscience 1998;82:1213–23. [PubMed: 9466441]

Rodriguez J, Specian V, Maloney R, Jourd'heuil D, Feelisch M. Performance of diamino fluorophores for the localization of sources and targets of nitric oxide. Free Radic Biol Med 2005;38:356–68. [PubMed: 15629864]

Rothe F, Canzler U, Wolf G. Subcellular localization of the neuronal isoform of nitric oxide synthase in the rat brain: a critical evaluation. Neuroscience 1998;83:259–69. [PubMed: 9466415]

Snyder SH, Ferris CD. Novel neurotransmitters and their neuropsychiatric relevance. Am J Psychiatry 2000;157:1738–51. [PubMed: 11058466]

Strijdom H, Muller C, Lochner A. Direct intracellular nitric oxide detection in isolated adult cardiomyocytes: flow cytometric analysis using the fluorescent probe, diaminofluorescein. J Mol Cell Cardiol 2004;37:897–902. [PubMed: 15380680]

Washko PW, Wang YH, Levine M. Ascorbic-acid recycling in human neutrophils. J Biol Chem 1993;268:15531–5. [PubMed: 8340380]

Wiesinger H. Arginine metabolism and the synthesis of nitric oxide in the nervous system. Prog Neurobiol 2001;64:365–91. [PubMed: 11275358]

Ye X, Kim WS, Rubakhin SS, Sweedler JV. Measurement of nitric oxide by 4,5-diaminofluorescein without interferences. Analyst 2004;129:1200–5. [PubMed: 15565218]

Zhang X, Kim WS, Hatcher N, Potgieter K, Moroz LL, Gillette R, Sweedler JV. Interfering with nitric oxide measurements. 4,5-diaminofluorescein reacts with dehydroascorbic acid and ascorbic acid. J Biol Chem 2002;277:48472–8. [PubMed: 12370177]

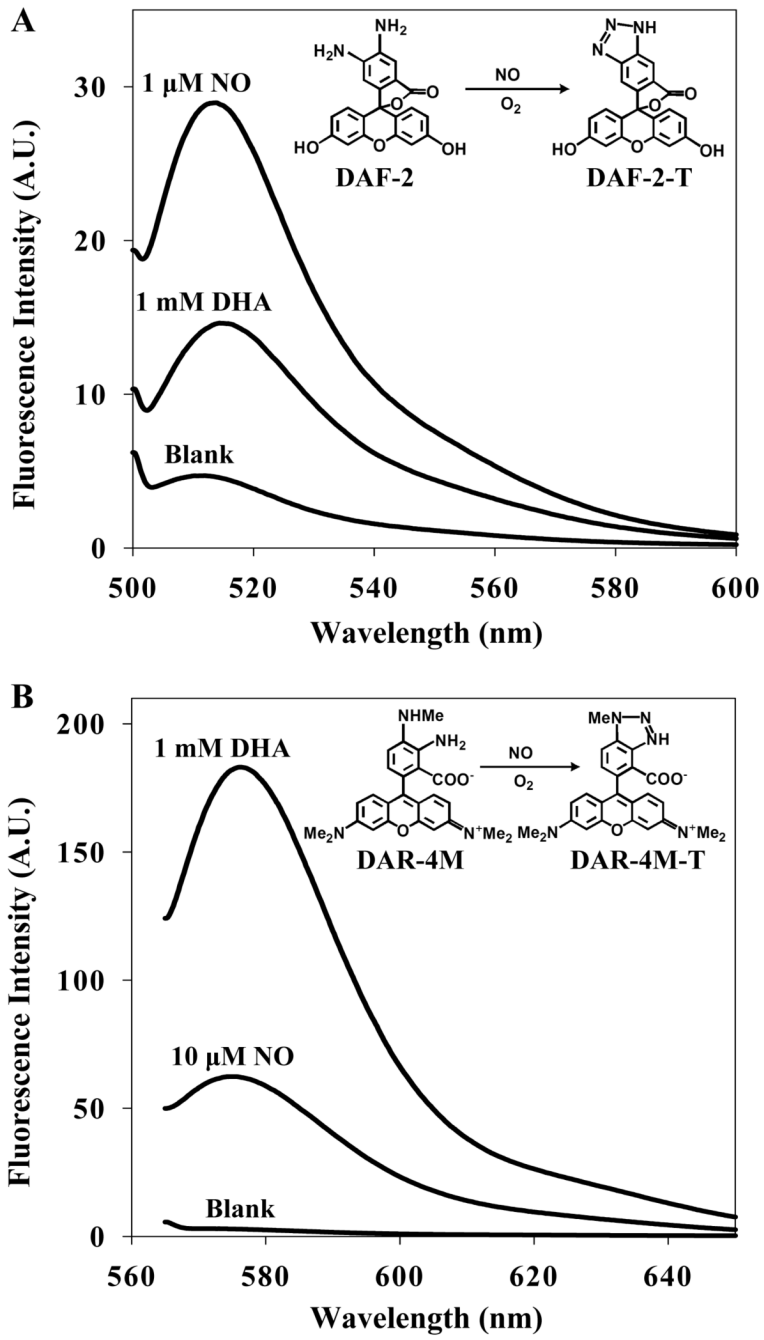

Fig. 1.

(A) Fluorescence emission spectra for 10 μM DAF-2 with 1 μM NO and 1 mM DHA. The blank contains 10 μM DAF-2 in phosphate buffer. (B) Fluorescence emission spectra for 10 μM DAR-4M with 10 μM NO and 1 mM DHA. The blank contains 10 μM DAR-4M in phosphate buffer.

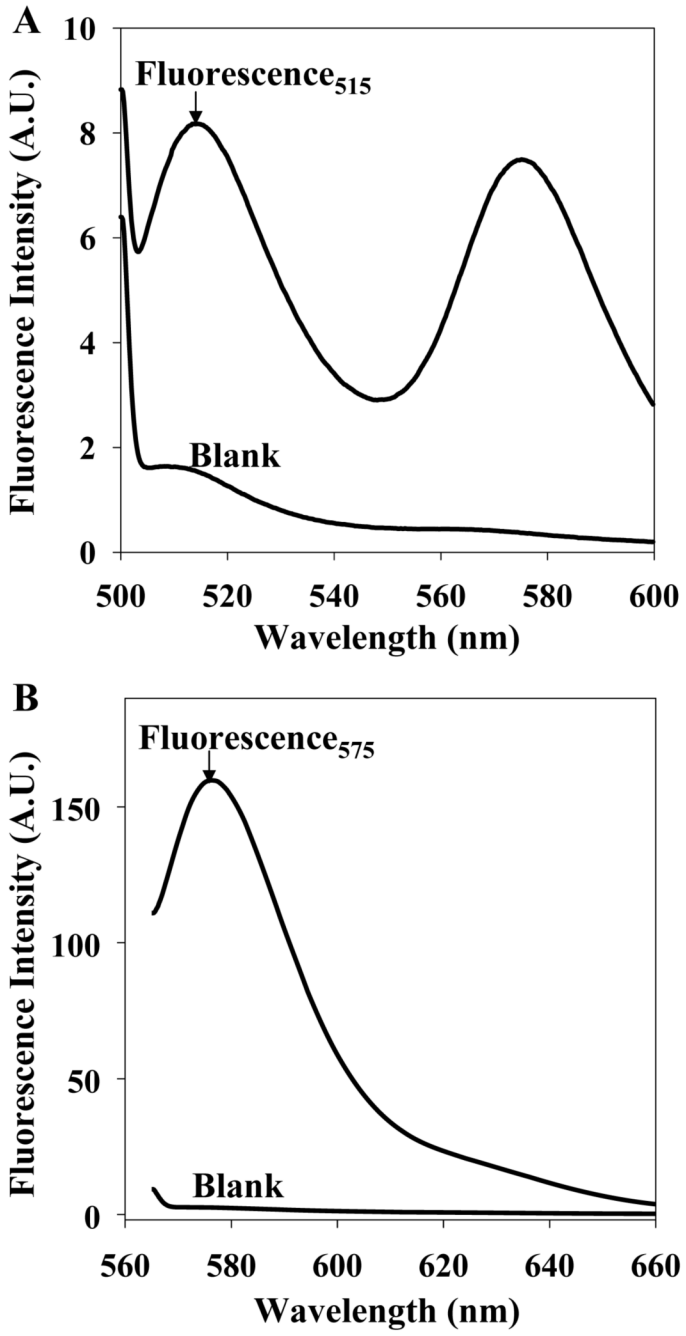

Fig. 2.

Fluorescence emission spectra for the mixture of 10 μM DAF-2 and 10 μM DAR-4M with 1 μM NO and 1 mM DHA measured (A) at 495 nm excitation and (B) at 560 nm excitation. The blank contains 10 μM DAF-2 and 10 μM DAR-4M in phosphate buffer.

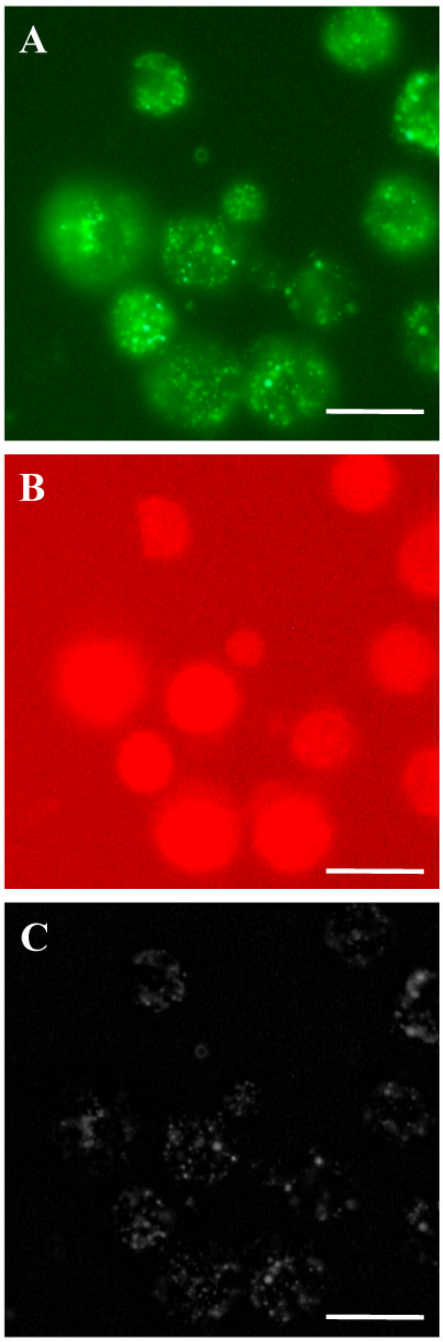

Fig. 3.

Fluorescence images of PC12 cells loaded with DAF-2 DA and DAR-4M AM. (A) Fluorescence image at an excitation of 450-490 nm. (B) Fluorescence image at an excitation of 515-560 nm. (C) Reconstructed image of NO concentration in PC12 cells. Scale bars, 100 μm.

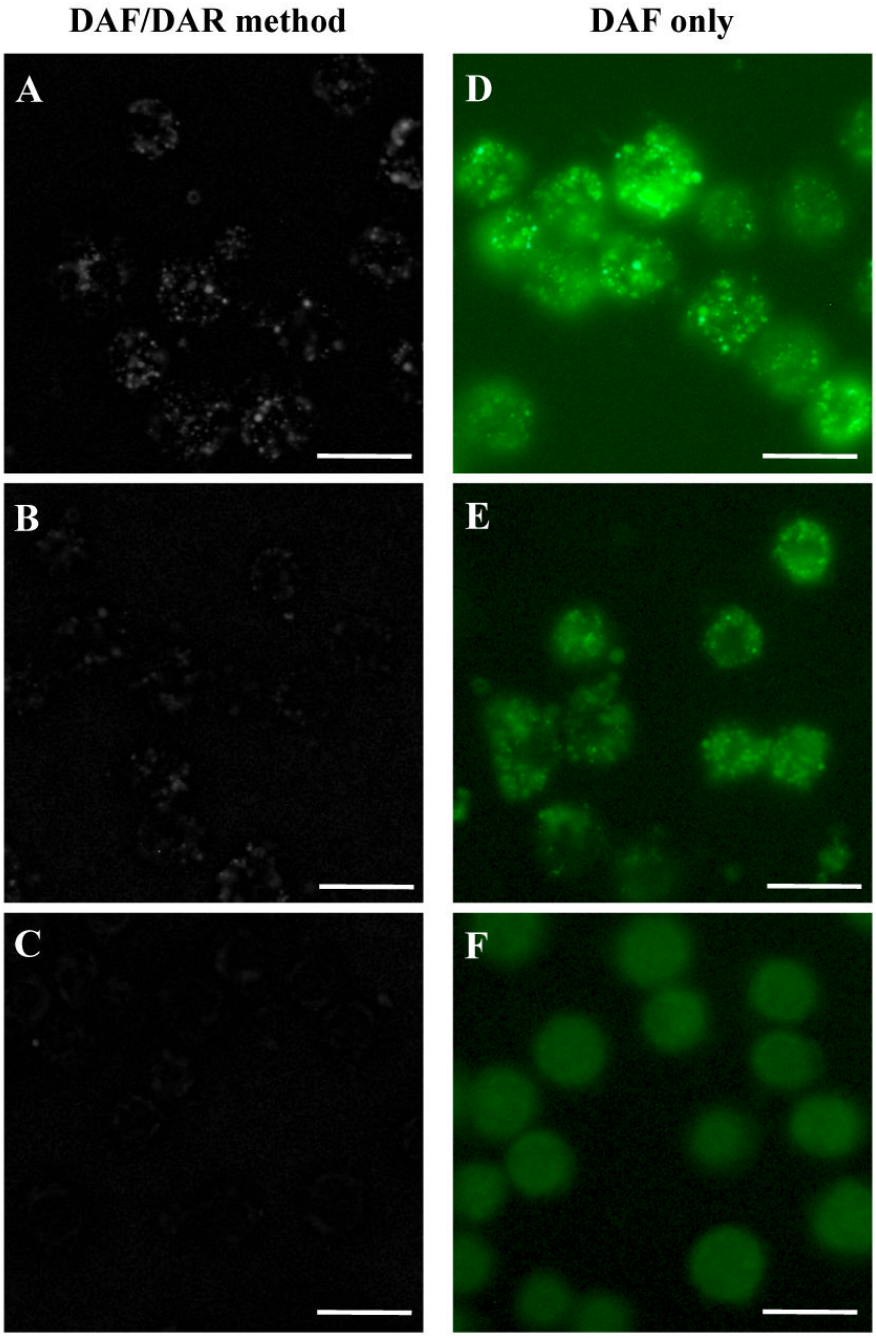

Fig. 4.

Comparison of fluorescence images obtained by the DAF/DAR ratiometric method (left column) and the commonly used DAF method (right column). (A, D) NO production was demonstrated in PC12 cells with no treatment, (B, E) in the presence of the NOS inhibitor, L-NAME, and (C, F) in the presence of the NO scavenger, carboxy-PTIO. Scale bars, 100 μm.

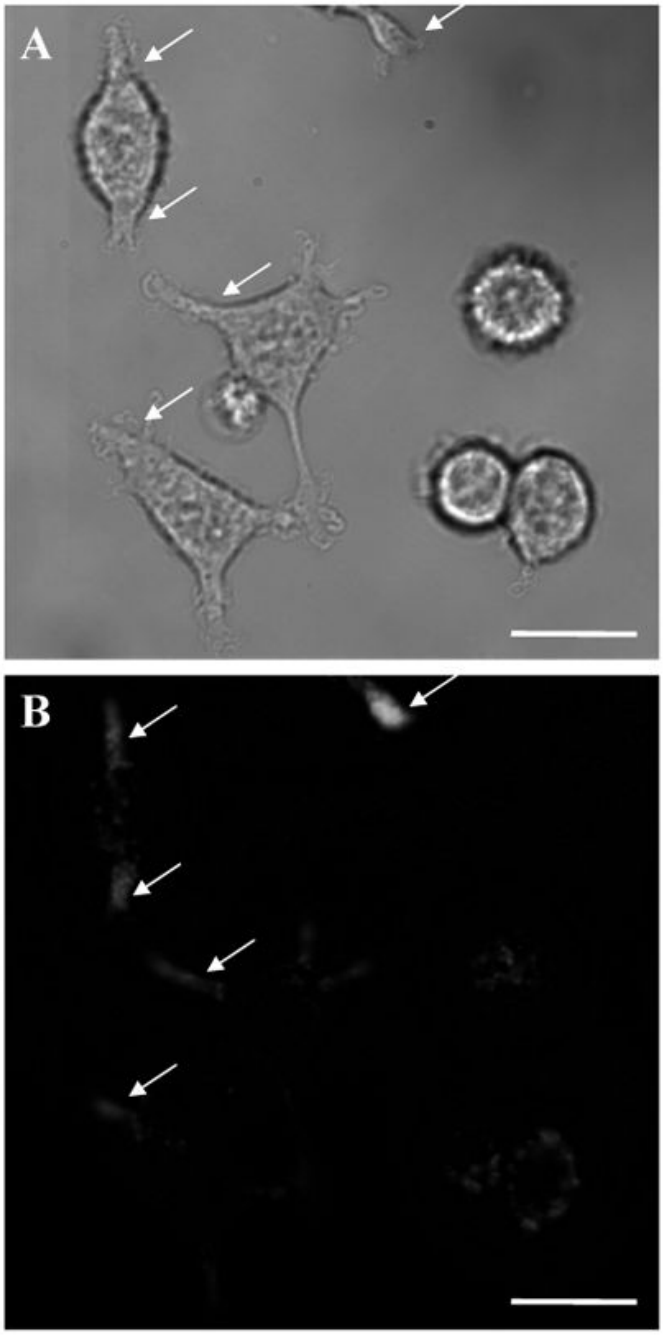

Fig. 5.
(A) Bright field image of differentiated PC12 cells. (B) Fluorescence image of NO production in differentiated PC12 cells (arrows) obtained by the DAF/DAR ratiometric method. Scale bars, 100 μm.

Table 1

Fluorescence intensity measured at emission wavelength of 515 nm upon 495 nm excitation, and at emission wavelength of 575 nm upon 560 nm excitation, in a series of standard solutions containing NO and DHA at different concentrations

NO Conc. (μM)	DHA Conc. (mM)	F_{515}	F_{575}
0	0	1.859	2.480
0.1	0.025	1.778	8.280
1	0.025	1.811	7.499
1	0.25	3.366	46.09
10	0.25	3.535	46.21
1	2.5	8.467	205.3
10	2.5	9.344	206.5